

Elastic and inclusive proton-proton scattering with bare-Pomeron intercept above 1*

S.-Y. Chu†, B. R. Desai, and B. C. Shen‡
University of California, Riverside, California 92502

R. D. Field
California Institute of Technology, Pasadena, California 91125
 (Received 6 November 1975)

An analysis of high-energy proton-proton scattering with bare-Pomeron intercept above 1 is presented. Using a value $\alpha_P(0)=1.06$, determined by the energy dependence of the pp total cross section, a triple-Regge analysis of the inclusive process $pp \rightarrow pX$ is carried out and compared with the results of a more conventional analysis with $\alpha_P(0)=1$. The resulting triple-Regge couplings are used in calculating the second-order corrections to the bare Pomeron in the bare perturbation expansion of Reggeon field theory. We find that such an approach can correctly describe the existing high-energy pp total-cross-section, elastic-, and inclusive-scattering data.

I. INTRODUCTION

The observed rising pp total cross section at Fermilab and CERN ISR has stimulated intense theoretical and phenomenological investigations regarding the nature of the Pomeron. In particular, much effort has gone into attempts to understand the behavior of pp total and elastic scattering using various models for the Pomeron¹⁻⁹ (e.g., optical, eikonal, geometric, multiperipheral, strong and weak cuts, etc.). However, because the total cross section, elastic scattering, diffractive resonance production, and inclusive $pp \rightarrow pX$ scattering are all related through unitarity; any effort to understand the Pomeron must inevitably involve a combined analysis of all four types of data.

Comparatively, little work has gone into the phenomenological understanding of the Pomeron in inclusive $p+p \rightarrow p+X$ scattering or diffractive resonance production. Previous triple-Regge analysis^{10,11} of $p+p \rightarrow p+X$ with $\alpha_P(0)=1$ attribute a rise in the pp total cross section to the summation over the mass of the X system and this rise is proportional to $G_{PPP}(0) \ln(\ln s)$, where $G_{PPP}(t)$ is the triple-Pomeron coupling. The magnitude of this coupling is, however, insufficient to produce the observed 4 mb rise of $\sigma_{\text{tot}}(pp)$ over the ISR region.^{11,12} In addition, diffractive resonance production, $pp \rightarrow pN^*$, is treated on a somewhat different footing from elastic $pp \rightarrow pp$ scattering. The elastic scattering is related via the optical theorem to the rising total cross section. The diffractive $pp \rightarrow pN^*$ production is related through FMSR (finite mass sum rules) and duality to the triple-Regge term PPP (abnormal duality) or PPR (normal duality) or a combination of the two

(mixed duality).¹³ In any case, with $\alpha_P(0)=1$ $\sigma(pp \rightarrow pN^*)$ would be expected to be constant or slightly decrease with energy and not rise like $\sigma_{\text{el}}(pp)$. Recent data on $N^*(1688)$ production^{14,15} show, however, that $\sigma(pp \rightarrow pN^*(1688))$ does indeed behave remarkably similar to $\sigma_{\text{el}}(pp)$.¹⁶ Thus it seems compelling to attempt to analyze the elastic, diffractive, and inclusive scattering in terms of the same type of bare-Pomeron singularity.

A framework within which one can describe both inclusive and exclusive scattering is the Reggeon field theory.¹⁷⁻¹⁹ It is a t -channel picture where the physical Pomeron is generated in terms of a bare-Pomeron and a triple-Pomeron coupling. In the weak-coupling solution the triple-Pomeron vertex vanishes at $t=0$ and both the bare and the physical Pomeron at $t=0$ are dominated by simple poles with unit intercept.²⁰ In the strong-coupling solution, the triple coupling does not vanish and the bare-Pomeron intercept is above 1. Here the physical Pomeron, obtained using the renormalization group and ϵ -expansion techniques, is now a cut giving the total cross section an s dependence of the form $(\ln s)^\eta$, $\eta > 0$, as $s \rightarrow \infty$.^{19,21,22}

Recent data²³ on inclusive $pp \rightarrow p+X$ scattering show no indication of a vanishing $G_{PPP}(t)$ for t as small as $|t|=0.035$ (GeV/c)². This, together with a rising $\sigma_{\text{tot}}(pp)$, favors the strong-coupling solution. The $(\ln s)^\eta$ behavior given by the strong-coupling solution for $\sigma_{\text{tot}}(pp)$ is, however, valid at asymptotic energies (i.e., at energies much higher than the highest available energy at ISR). At presently available energies the bare perturbation expansion should be used to compare theory with data.²¹

We perform a triple-Regge analysis of inclusive

$pp \rightarrow pX$ scattering with bare-Pomeron intercept greater than 1. The value used for the intercept is $\alpha_P(0) = 1.06$ which is determined from the energy dependence of the pp total cross section. We compare the features of this type of solutions with those with the usual $\alpha_P(0) = 1$. Then, using the determined triple-Regge couplings and the bare perturbation expansion to second order [Fig. 1(a)] we attempt to describe the Pomeron contributions to pp scattering. In our analysis of pp elastic scattering and total cross section we will confine ourselves to the region $500 \leq s \leq 3000$ GeV/ c and will thus ignore the contributions of all secondary Regge trajectories except where they couple to the Pomeron through the triple-Regge couplings.

We interpret the first two terms in the bare-Pomeron perturbation expansion in terms of an s -channel picture.²⁴ The bare Pomeron [first term in Fig. 1(a)] can be identified as being generated by the (rapidly converging) multiperipheral series owing to non-Pomeron Regge exchanges with low rapidity gaps. The second term then represents absorptive corrections provided by the contributions of the various intermediate states $p + p \rightarrow X_1 X_2$ including the elastic state, with X_1 and X_2 separated by a large rapidity gap [see Fig. 1(b)]. In other words, one can identify the first two terms of the expansion as an expansion in the rapidity gap length (fireball expansion).²⁵ The crucial absorptive sign corresponds to using Gribov's prescription for evaluating the cut.¹⁷ In making such an identification we have used duality for the Pomeron-particle amplitude to include the elastic along with the higher-mass intermediate states.²⁴

One advantage of the s -channel picture is that one can include the s -channel threshold factors so that at a given energy only a finite number of terms in the expansion are nonzero. The presence of such threshold factors may be useful for understanding the transition from finite s where the bare expansion holds to the asymptotic s where the cut dominates.²⁶ In addition, the s channel is the most convenient description when discussing absorptive-type models.

The terms higher than the second order are quite complicated and so is their s -channel interpretation. Furthermore, as $s \rightarrow \infty$ more and more terms in the perturbation expansion will be significant and the strong-coupling results of the Reggeon calculus indicate that the bare perturbation expansion will eventually break down. Therefore, at finite s the perturbation expansion would be useful if only a finite number of terms are important. We find that the first two terms are adequate in describing many features of the pres-

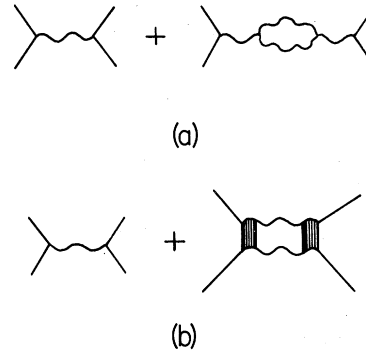


FIG. 1. First two terms of the bare-Pomeron perturbation expansion are given by (a). The second term in (a) represents absorptive corrections, as given by (b), provided by the contributions of the various intermediate states $pp \rightarrow X_1 + X_2$ including the elastic state, with X_1 and X_2 separated by a large rapidity gap.

ent data.

In Sec. II we discuss the theoretical formalism used to analyze the pp total cross section, pp elastic scattering, and the inclusive process $pp \rightarrow p + X$. In Sec. III we perform a triple-Regge analysis of the inclusive process $pp \rightarrow p + X$, using a bare-Pomeron intercept appropriate for the rising pp total cross section [$\alpha_P(0) = 1.06$]. These results are compared with more conventional fits with $\alpha_P(0) = 1$. The differential elastic and total pp cross sections are analyzed in Sec. IV using the triple-Regge coupling obtained from the inclusive analysis. We present a summary and conclusions in Sec. V. In addition we have relegated some of the detailed calculations to Appendixes A, B, and C.

II. FORMALISM

In this section we display the relevant formulas for the pp total cross-section, elastic, and $pp \rightarrow p + X$ inclusive scattering. For the elastic case we consider only the non-helicity-flip amplitude and in addition we attempt to write the various formulas with as few arbitrary parameters as possible. The derivations and approximations are discussed in detail in Appendixes A, B, and C.

We first write down the bare-Pomeron term, then the triple-Regge terms, followed by the bubble terms.

A. Bare-Pomeron term

This is the first term in Figs. 1(a), 1(b). In the s -channel picture, as we discussed in the Introduction, it can be considered as a sum of a rapidly converging multiperipheral series owing to the

exchange of non-Pomeron trajectories with low rapidity gaps. It is a simple pole in the j plane:

$$\frac{f_1(t)}{j - \alpha_P(t)}, \quad (2.1)$$

with

$$\alpha_P(t) = 1 + \epsilon + \alpha'_P t, \quad \epsilon > 0. \quad (2.2)$$

Its s -channel projection is given by

$$f_1(t) s^{\alpha_P(t)}. \quad (2.3)$$

The residue function, $f_1(t)$, is expressed in the exponential form as

$$f_1(t) = f_1 e^{2a_1 t}, \quad (2.4)$$

where the t dependence of the residue is discussed in Appendix A.

B. Triple-Regge couplings

The term $g_{ijk}(t) = g_{ijk}(t, t, 0)$ (see Appendix A) denotes the triple-Regge coupling of the three reggeons i , j , and k , where Regge poles i and j with trajectories $\alpha_i(t)$, $\alpha_j(t)$, respectively, are exchanged and Regge pole k with trajectory $\alpha_k(0)$ controls the Reggeon-particle total cross section as shown in Fig. 2. The triple-Regge formula for $pp \rightarrow p + X$ inclusive scattering is then given by

$$s \frac{d\sigma}{dt dM^2} (p + p \rightarrow p + X) = \frac{1}{s} \sum_{ijk} G_{ijk}(t) \left(\frac{s}{\nu}\right)^{\alpha_i(t) + \alpha_j(t)} \nu^{\alpha_k(0)}, \quad (2.5)$$

where $t = M^2 - t - m_p^2$ and where we have lumped together into $G_{ijk}(t)$ the triple-Regge coupling $g_{ijk}(t)$ [Fig. 3(a)] and the three Reggeon-particle vertices $F_i(t)$, $F_j(t)$, and $F_k(0)$ [Fig. 3(b)] and

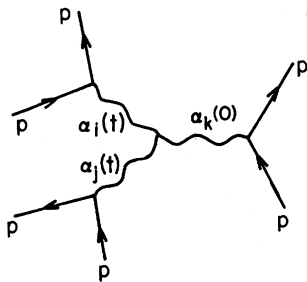


FIG. 2. Diagram corresponding to the triple-Regge region for the inclusive process $pp \rightarrow p + X$.

the appropriate signature factors ξ_i , namely

$$G_{ijk}(t) = (1/16\pi) F_i(t) F_j(t) F_k(0) g_{ijk}(t) \xi_i \xi_j^*, \quad (2.6)$$

We parametrize the couplings $G_{ijk}(t)$ as follows:

$$G_{ijk}(t) = \lambda_1 e^{\mu_1 t} + \lambda_2 e^{\mu_2 t}, \quad (2.7)$$

where the subscripts ijk have been suppressed in the λ 's and μ 's. A single exponential is insufficient in fitting both small- $|t| \leq 0.5$ (GeV/c)² and large- $|t|$ [$|t| \geq 0.5$ (GeV/c)²] data.

C. Bubble terms

These correspond to the second term in Fig. 1(a), and involve the product $g_{ijk} g_{i'j'k'}$ [see Fig. 3(c)]. We will divide these products into two categories, one without interference terms and one with. We, of course, exclude those terms which do not communicate with the $I=0$ crossed channel (e.g., $g_{PP\pi} g_{PP\pi}$, etc.).

(i) *Noninterference terms.* By this we mean $i=j$, and $k'=k$.

(a) $(PPP)^2$. Here $i=j=P$, $k'=k=P$ and involve g_{PPP}^2 . The contribution of this term to the elastic amplitude is discussed in detail in Appendixes B and C. It is written as²⁷

$$g_{PPP}^2(0) e^{2c_P t} \frac{s^{\alpha_c(t)}}{2\alpha'_P \ln s} \times \left[\frac{(rs)^{[\alpha_P(t) - \alpha_c(t)]/2} - (M_0^2)^{\alpha_P(t) - \alpha_c(t)}}{\alpha_P(t) - \alpha_c(t)} \right]^2, \quad (2.8)$$

where $\alpha_c(t)$ is the Pomeron-Pomeron cut trajectory

$$\alpha_c(t) = 1 + 2\epsilon + \frac{1}{2} \alpha'_P t. \quad (2.9)$$

(b) $(PPR)^2$. Here $i=j=P$, $k=k'=R$ and involves g_{PPR}^2 . This term is also discussed at length in Appendixes B and C. Its contribution to the elastic amplitude is written as²⁷

$$g_{PPR}^2(0) e^{2c_R t} \frac{s^{\alpha_c(t)}}{2\alpha'_P \ln s} \times \left[\frac{(rs)^{[\alpha_R(t) - \alpha_c(t)]/2} - (M_0^2)^{\alpha_R(t) - \alpha_c(t)}}{\alpha_R(t) - \alpha_c(t)} \right]^2 \quad (2.10)$$

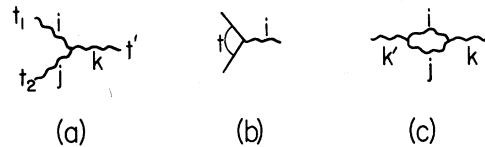


FIG. 3. (a) Triple-Regge vertex $g_{ijk}(t_1, t_2, t')$; (b) Reggeon-particle coupling $F_i(t)$; (c) bubble term corresponding to $g_{ijk} g_{i'j'k'}$.

(c) $(\pi\pi P)^2$ and $(RRP)^2$. These pion and Reggeon bubble terms correspond to large rapidity gap events. The pion bubble term, because it involves the pion propagator, will give rise to a very sharp falloff near $t=0$. From the triple-Regge analysis to be discussed in Sec. III below, the $\pi\pi P$ contribution is not negligible. We expect therefore that it will be responsible for the observed break at $t \approx -0.1$ (GeV/c)² in the elastic differential cross section. For our purposes here, we combine the $(\pi\pi P)^2$ term with the Reggeon bubble term $(RRP)^2$. The sum can be approximated phenomenologically as a single exponential term which will add to the pole contribution (see Appendix B)²⁸:

$$f_2 e^{2a_2 t} s^{\alpha_P(t)}. \quad (2.11)$$

$$T(s, t) = - (f_1 e^{2a_1 t} + f_2 e^{2a_2 t}) (s e^{-i\pi/2})^{\alpha_P(t)} + \frac{16\pi}{2.5 f_1^2} G_{PPP}^2(0) e^{2c_P t} \frac{(s e^{-i\pi/2})^{\alpha_c(t)}}{2\alpha'_P \ln(s e^{-i\pi/2})} \left[\frac{(\gamma s e^{-i\pi/2})^{[\alpha_P(t) - \alpha_c(t)]/2} - M_0^2}{\alpha_P(t) - \alpha_c(t)} \right]^2 + \frac{16\pi}{2.5 f_1^2} G_{PPR}^2(0) e^{2c_R t} \frac{(s e^{-i\pi/2})^{\alpha_c(t)}}{2\alpha'_P \ln(s e^{-i\pi/2})} \left[\frac{(\gamma s e^{-i\pi/2})^{[\alpha_R(t) - \alpha_c(t)]/2} - (M_0^2)^{\alpha_R(t) - \alpha_c(t)}}{\alpha_R(t) - \alpha_c(t)} \right]^2, \quad (2.12)$$

$$\sigma_{\text{tot}} = \frac{1}{s} \text{Im} T(s, t=0), \quad (2.13)$$

$$\frac{d\sigma_{\text{el}}}{dt} = \frac{2.5}{16\pi s^2} |T|^2, \quad (2.14)$$

$$s \frac{d\sigma(p+p \rightarrow p+X)}{dt dM^2} = \frac{1}{s} \sum_{ijk} G_{ijk}(t) \left(\frac{s}{\nu}\right)^{\alpha_i(t) + \alpha_j(t)} (\nu)^{\alpha_k(0)}, \quad (2.15)$$

where $\nu = M^2 - t - m_p^2$ and the scale factor is taken to be 1 GeV², and where $\alpha_P(t) = 1 + \epsilon + \alpha'_P t$ and $\alpha_c(t) = 1 + 2\epsilon + \frac{1}{2}\alpha'_c t$.

III. TRIPLE-REGGE ANALYSIS OF $p+p \rightarrow p+X$

A bare-Pomeron intercept above 1 is consistent with a rising total cross section.^{5,6} As discussed in Sec. IV, a value of $\alpha_P(0) = 1.06$ correctly describes the energy dependence of the total cross section. Whether such an intercept is compatible with pp inclusive data, however, requires careful examination. In this section we update the triple-Regge and finite-mass-sum-rule analysis of the inclusive reaction $pp \rightarrow p+X$ performed earlier by Field and Fox¹¹ (hereafter referred to as *FF*) by including recent Fermilab data. We compare triple-Regge solutions with $\alpha_P(0) = 1.06$ with a more conventional analysis with $\alpha_P(0) = 1$.

(ii) *Interference terms.* These involve terms such as g_{PRP}^2 , where $i \neq j$ but $k' = k$, and $g_{PPP} g_{PPR}$, where $i = j$ but $k' \neq k$. We will ignore the interference terms involving $i \neq j$ (e.g., g_{PRP}) throughout our entire analysis involving elastic as well as inclusive scattering. As far as other interference terms are concerned we note that they do not give rise to any additional structure either in s or t than what is already present in the terms we discussed earlier. Therefore, their contributions will not be parametrized separately.

D. Summary of formulas

The full expressions for the elastic pp amplitude $T(s, t)$ the total cross section σ_{tot} the elastic differential cross section $d\sigma_{\text{el}}/dt$, and the inclusive cross section are given by

A. Data base

We include in our triple-Regge fits all the high-energy $p+p \rightarrow p+X$ inclusive data given in Table II of *FF* with the following exceptions:

(i) The 300-GeV/c data from the Stony Brook-Columbia collaboration²⁹ have been deleted. These data showed a dipping of $s d\sigma/dt dM^2$ at small $|t|$ for $8 \leq M^2 \leq 12$ GeV² (see Fig. 13 of *FF*), which was erroneous.³⁰ Newer data from this group and others show no indication of a dip in the inclusive cross section at small $|t|$ (see Fig. 4).³¹

(ii) We have included the recent data from the Dubna-Fermilab-Rockefeller-Rochester Collaboration²³ on $p+d \rightarrow d+X$ which have been converted to $p+p \rightarrow p+X$ by division of the deuteron form factor. These data were taken at $p_{\text{lab}} = 150, 210, 260, 275,$ and 385 GeV/c for a mass range $0 \leq M^2 \leq 30$ GeV² and small $|t|$ [$0.035 \leq |t| \leq 0.115$ (GeV/c)²].

(iii) We have included recent data from the ISR asymmetrical beam experiment performed at $s = 551, 720, 930,$ and 1490 GeV^2 by the CHLM collaboration.³² This group has $p+p \rightarrow p+X$ data at $t = -0.25, -0.35,$ and -0.50 with $M^2 = 30 \text{ GeV}^2$.

We do not explicitly fit the FMSR data from FF but we check to see that our solutions are consistent with the FMSR.

B. Parametrizations

In the inclusive analysis only the bare pole terms are kept; the bubble terms are ignored. We varied

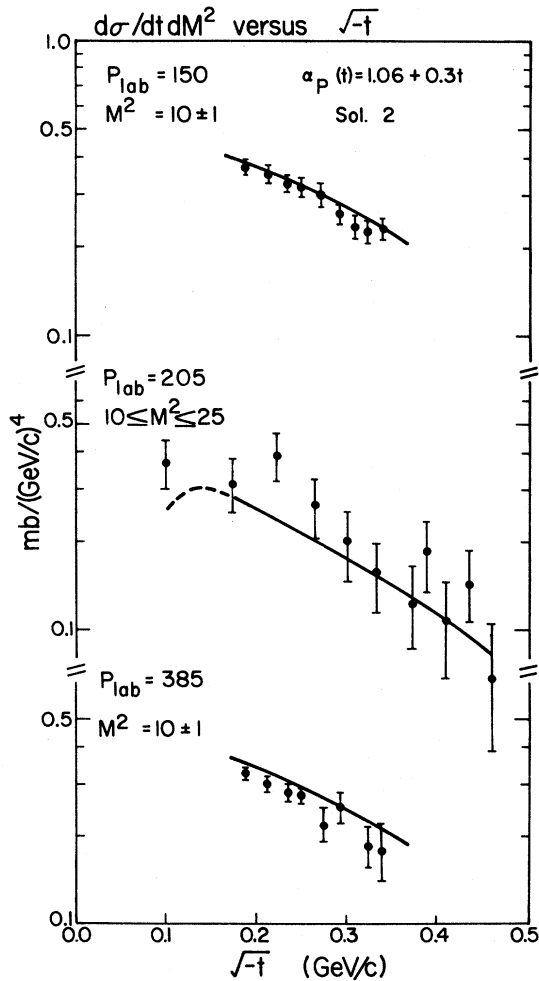


FIG. 4. Small- $|t|$ data for $d\sigma/dt dM^2$ ($pp \rightarrow p+X$) versus $\sqrt{-t}$ at $p_{\text{lab}} = 150$ and $385 \text{ GeV}/c$ (Ref. 23) and $p_{\text{lab}} = 205 \text{ GeV}/c$ (Ref. 45). The data at 150 and $385 \text{ GeV}/c$ are $pd \rightarrow d+X$ which have been converted to $pp \rightarrow p+X$ by suitable division by the deuteron form factor. The curves are the result of Solution 2 with $\alpha_P(t) = 1.06 + 0.3t$. The turnover in the $205\text{-GeV}/c$ data is a t_{min} effect and not connected to the turnover of any triple-Regge terms.

the triple-Regge couplings $G_{ijk}(t)$ in Eq. (2.5) in an attempt to fit the high-energy inclusive $pp \rightarrow p+X$ data discussed above (3.1). The couplings were parametrized by Eq. (2.7) with trajectories

$$\alpha_R(t) = 0.5 + t, \quad (3.1a)$$

$$\alpha_\pi(t) = t, \quad (3.1b)$$

$$\alpha_P(t) = 1 + \epsilon + \alpha_P' t. \quad (3.1c)$$

There has been some question in the past as to whether or not the triple-Pomeron coupling $G_{PPP}(t)$ vanishes at $t=0$ (see discussion in FF). Recent data on $d\sigma/dt dM^2$ show no indication of a dipping at small $|t|$ (see Fig. 4). We thus parametrize $G_{PPP}(t)$ to be nonzero at $t=0$ [Eq. (2.7)]. In addition, there is evidence of some slight Pomeron shrinkage in inclusive $pp \rightarrow p+X$ scattering (Fig. 5). A Pomeron slope $\alpha_P' = 0.3 (\text{GeV}/c)^{-2}$ is consistent with this data.

We present two solutions: Solution 1 with $\epsilon = 0$, which is a slightly different version of FF Solution 1 (using a new data base), and the new solution, Solution 2, with $\epsilon = 0.06$. The choice of $\epsilon = 0.06$ is determined mainly by the total and differential elastic data (see Sec. IV below).

Solution 1: This solution contains no interference terms, has $\alpha_P(0) = 1.0$ and has a nonvanishing triple-Pomeron coupling at $t=0$. The PPP, PPR, RRP are parametrized according to (2.7) and var-

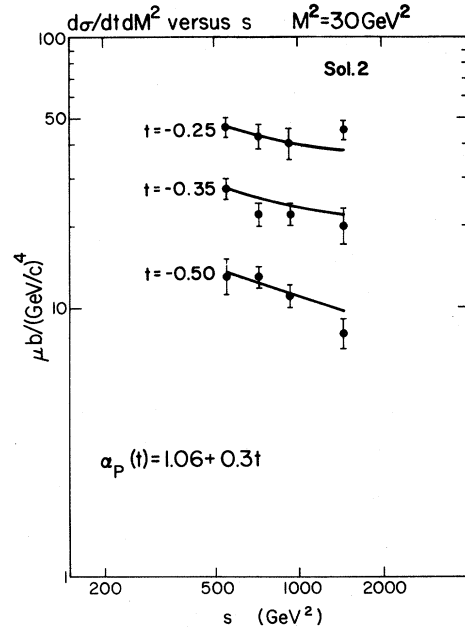


FIG. 5. Data on $d\sigma/dt dM^2$ versus s for $pp \rightarrow p+X$ at $M^2 = 30 \text{ GeV}^2$ (Ref. 32). The curves are the result of Solution 2 (normalized up by 20%) with $\alpha_P(t) = 1.06 + 0.3t$.

TABLE I. Triple-Regge couplings $G_{ijk}(t) = \lambda_1 e^{\mu_1 t} + \lambda_2 e^{\mu_2 t}$. For *PPP* and *RRP*, λ_1 and λ_2 are given in units of $\text{mb}/(\text{GeV}/c)^2$; for *PPR* and *RRR*, λ_1 and λ_2 are given in units of $\text{mb}/(\text{GeV}/c)$. μ_1 and μ_2 are given in units of $(\text{GeV}/c)^{-2}$.

	$\alpha_P(0)=1.0$		$\alpha_P(0)=1.06$	
	λ_1, λ_2	μ_1, μ_2	λ_1, λ_2	μ_1, μ_2
<i>PPP</i>	2.59, 0.34	4.02, 0.90	1.24, 0.32	3.49, 1.54
<i>PPR</i>	2.41, 0.021	2.66, -1.49	0.922, 0.017	3.075, -1.6
<i>RRP</i>	18.5, 1.91	3.37, -2.20	11.35, 1.69	5.53, -2.44
<i>RRR</i>	18.1	12.0	83.7	2.95
α'_P [$(\text{GeV}/c)^{-2}$]	0.29		0.30	
χ^2	2623		2436	

ied. The *RRR* term is fixed at the value given by Solution 1 of FF. In addition, the $\pi\pi P$ and $\pi\pi R$ terms are estimated as in FF. Namely,

$$G_{\pi\pi P}(t) = \frac{1}{4\pi} \frac{g_{\pi\pi P}^2}{4\pi} \sigma_{\text{tot}}^P(\pi^0 p) \frac{(-t)e^{b_\pi(t-\mu^2)}}{(t-\mu^2)^2}, \quad (3.2a)$$

$$G_{\pi\pi R}(t) = \frac{1}{4\pi} \frac{g_{\pi\pi R}^2}{4\pi} \sigma_{\text{tot}}^R(\pi^0 p) \frac{(-t)e^{b_\pi(t-\mu^2)}}{(t-\mu^2)^2}, \quad (3.2b)$$

where the $\pi^0 p$ total cross section is given by

$$\sigma_{\text{tot}}(\pi^0 p) = \sigma_{\text{tot}}^P(\pi^0 p) + \sigma_{\text{tot}}^R(\pi^0 p)/\sqrt{s}, \quad (3.2c)$$

and where $g_{\pi\pi P}^2/4\pi \approx 14.5$, $\sigma_{\text{tot}}^P(\pi^0 p) = 21.3$ mb, $\sigma_{\text{tot}}^R(\pi^0 p) = 19.7$ mb GeV. For simplicity we take $b_\pi = 0$ as in FF.

Solution 2: This solution contains no interference terms and has $\alpha_P(t) = 1.06 + 0.3t$, and has a nonvanishing triple-Pomeron coupling at $t=0$. The *PPP*, *PPR*, and *RRP* terms are varied and are parametrized according to (2.7). In addition the *RRR* term is parametrized by

$$G_{RRR}(t) = \lambda e^{\mu t}, \quad (3.3)$$

and allowed to vary. The $\pi\pi P$ and $\pi\pi R$ terms are given by (3.1a) and (3.1b), but this time with

$$\sigma_{\text{tot}}(\pi^0 p) = \sigma_{\text{tot}}^P(\pi^0 p) s^{0.06} + \sigma_{\text{tot}}^R(\pi^0 p)/\sqrt{s}, \quad (3.2d)$$

where $\sigma_{\text{tot}}^P(\pi^0 p) = 15.0$ mb and $\sigma_{\text{tot}}^R(\pi^0 p) = 34.5$ mb GeV (we take $b_\pi = 0$ as in Solution 1).

The resulting triple-Regge couplings for Solutions 1 and 2 are given in Table I and shown in Fig. 6. When discussing various solutions it is useful to compare the cosmic triple-Regge parameters $C_{ijk}(s, M^2)$ defined in Ref. 12 and used by FF:

$$C_{ijk}(s, M^2) = \int_{-1}^0 (d\sigma/dt dM^2)_{ijk} dt s^2 \times \left(\frac{M^2}{s}\right)^{\alpha_i(0) + \alpha_j(0)} / (M^2)^{\alpha_k(0)}, \quad (3.4)$$

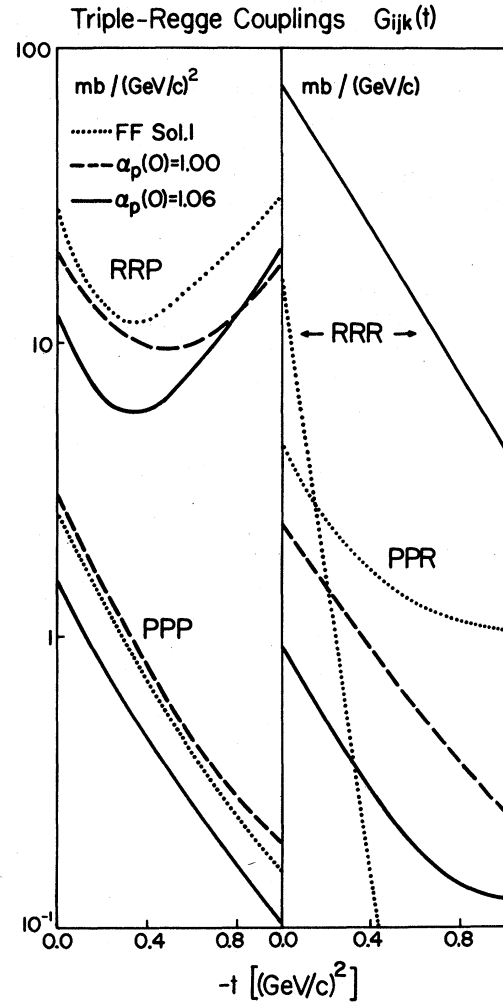


FIG. 6. Comparison of the various triple-Regge couplings $G_{ijk}(t)$ arising from our Solution 1 [$\alpha_P(0)=1.0$] and Solution 2 [$\alpha_P(0)=1.06$] and Solution 1 of Field and Fox (FF, Ref. 11).

where ijk labels the triple-Regge term. These parameters are such that when multiplied by the cosmic kinematic factor recorded in Table II, they give the value of the integral

$$\int_{-1}^0 (d\sigma/dt dM^2) dt.$$

The cosmic parameters resulting from solutions 1 and 2 are compared with Solution 1 of FF in Table II.

C. Comparison of Solution 1 ($\epsilon = 0$) with FF Solution 1

As can be seen from Fig. 6 the primary difference between these two solutions is that our Solution 1 has a smaller PPR term (by about a factor of 2). This is due to the removal of the Stony Brook-Columbia 300-GeV/c data³⁰ which required a sizeable $1/M^3$ component to fit the shape of the mass spectra (see Fig. 8 of FF) and to the inclusion of the new Dubna-Fermilab data,²³ which show little $1/M^3$ component. In fact these new data show $M^2 d\sigma/dt dM^2$ to be roughly flat when plotted versus M^2 for $10 \leq M^2 \leq 30$ GeV² and $|t| = 0.035$ (GeV/c)², indicating mostly PPP and little PPR (see Fig. 7).³³⁻³⁵ This is confirmed by the fact that at this t value $s d\sigma/dt dM^2$ very nearly scales (independent of s) when plotted versus x (Fig. 7). A PPR contribution is, however, definitely needed at $|t| = 0.16$ (GeV/c)² to produce the amount of nonscaling seen by Sannes *et al.*,³⁶ (Figs. 8 and Fig. 9), and in fact our fit results in a non-negligible PPR even at $|t| = 0.035$ (GeV/c)² (Fig. 10). The fit also has a small RRP term at

$|t| = 0.035$ (GeV/c)² producing a slight rise in $M^2 d\sigma/dt dM^2$ as M^2 increases, which is perhaps seen in the data.

D. Comparison of Solution 1 ($\epsilon = 0$) with Solution 2 ($\epsilon = 0.06$)

The size of $G_{PPP}(t)$ is decreased when going from Solution 1 to Solution 2; however, as can be seen from Fig. 6 the magnitudes of the over-all PPP contribution at $|t| = 0.035$ (GeV/c)² and $p_{lab} = 385$ GeV/c are almost identical. One main difference between these two solutions is that Solution 2 has a smaller PPR term and a considerably larger RRR contribution. The reasons for this can be understood by studying Fig. 9 where we display the various contributions to $s d\sigma/dt dM^2$ versus $1/\sqrt{s}$ for $t = -0.16$ (GeV/c)² and $x = 0.91$. Figure 8 shows that there is a certain amount of energy dependence in the data to be accounted for by the triple-Regge terms. In Solution 1 [$\alpha_P(0) = 1.0$] the terms PPP , RRP , and $\pi\pi P$ roughly scale (independent of s at fixed x) and the nonscaling seen in the data is accounted for primarily by PPR . On the other hand, for Solution 2 [$\alpha_P(0) = 1.06$] the PPP , RRP , and $\pi\pi P$ terms do *not* scale. They, in fact, increase with increasing s at fixed x , which must be compensated for by a large amount of $PPR + RRR$. The solution does this by increasing greatly the size of the RRR term. Solution 2 has the interesting property that eventually $s d\sigma/dt dM^2$ will rise as the energy is increased at fixed x , rather than decrease to a scaling limit.

TABLE II. Cosmic triple-Regge parameters $C_{ijk}(s, M^2)$ [defined in (3.4)], where $\alpha_P(0) = 1 + \epsilon$, $\alpha_R(0) = \frac{1}{2}$, and $\alpha_\pi(0) = 0$. When multiplied by the cosmic kinematic factors in the first column (in GeV units), the parameters give the value of

$$\int_{-1}^0 (d\sigma/dt dM^2) dt$$

in mb/GeV².

	Cosmic kinematic factor	FF Solution 1	$\alpha_P(0) = 1.00$ Solution 1	$\alpha_P(0) = 1.06$ Solution 2
PPP	$s^2 \epsilon / (M^2)^{1+\epsilon}$	0.498, 0.445	0.591, 0.534	0.338, 0.304
PPR	$M^{-3} (s/M^2)^2 \epsilon$	0.977, 0.851	0.590, 0.527	0.215, 0.192
RRP	$(M^2)^\epsilon / s$	3.18, 2.59	2.49, 2.00	1.46, 1.17
RRR	$1/(sM)$	1.03, 0.94	1.03, 0.94	9.60, 7.97
$\pi\pi P$	$(M^2)^{1+\epsilon} / s^2$	27.4, 23.3	27.4, 23.3	19.3, 16.4
$\pi\pi R$	M/s^2	25.1, 21.3	25.1, 21.3	45.3, 38.5
p_{lab} (GeV/c)		200, 500	200, 500	200, 500
M^2 (GeV ²)		20	20	20
ϵ		0.0	0.0	0.06

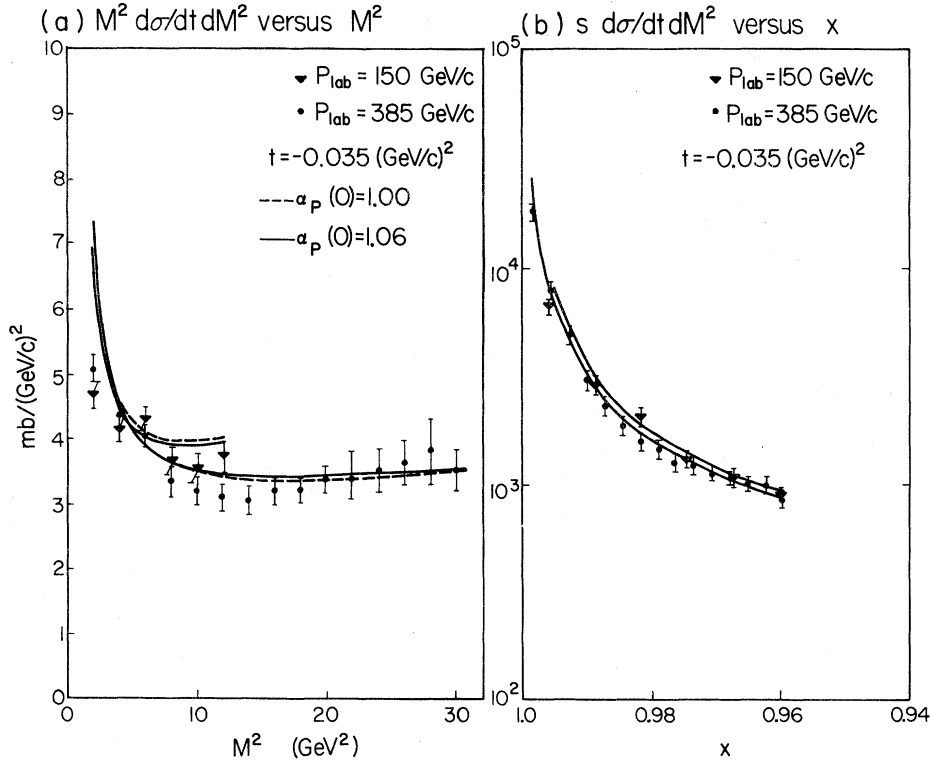


FIG. 7. Data on $M^2 d\sigma/dtdM^2$ versus M^2 [diagram (a)] and $s d\sigma/dtdM^2$ versus x [diagram (b)] at $t = -0.035$ (GeV/c) 2 and $p_{\text{lab}} = 150$ and 385 (GeV/c) 2 . This data for $pp \rightarrow p + X$ has been arrived at from $pd \rightarrow d + X$ by suitable division by the deuteron form factor (Ref. 23). The curves are the results of Solution 1 [dashed; $\alpha_P(0) = 1$] and Solution 2 [solid; $\alpha_P(0) = 1.06$].

E. Inelastic diffraction cross section

Owing to the Pomeron intercept being greater than 1 Solution 2 produces an inelastic diffractive cross section which rises substantially with increasing energy. Explicitly, defining an inelastic diffractive cross section by (we use $r = 0.2$ here instead of $r = 0.1$ in order to compare with Solution 1 of FF)

$$\sigma_D(s) = \frac{2}{s} \int_2^{0.2s} dM^2 \times \int_{-\infty}^{t_{\text{min}}} dt \left[G_{PPP}(t) \left(\frac{\nu}{s} \right)^{1 + \epsilon - 2\alpha_P(t)} + G_{PPR}(t) \left(\frac{\nu}{s} \right)^{1/2 - 2\alpha_P(t)} 1/\sqrt{s} \right] \quad (3.5)$$

F. Diffractive resonance production duality

Assuming semilocal duality one can relate triple-Regge couplings PPP and PPR to diffractive resonance production as follows¹⁶:

$$\frac{d\sigma}{dt} (pp \rightarrow pN^*) \approx \frac{2}{s^2} \frac{1}{\nu_R} \int_{\nu_1}^{\nu_2} d\nu \nu \left[(1-d) G_{PPP}(t) \left(\frac{s}{\nu} \right)^{2\alpha_P(t)} \nu^{\alpha_P(0)} + d G_{PPR}(t) \left(\frac{s}{\nu} \right)^{2\alpha_P(t)} \nu^{\alpha_R(0)} \right], \quad (3.6)$$

results in the values given in Table III of $p_{\text{lab}} = 300$ and 1500 GeV/c for Solutions 1 and 2 and Solution 1 of FF. Solution 2 produces almost a 2 mb rise over this energy region (see Fig. 11), whereas solutions with $\alpha_P(0) = 1.0$ have less than a 1 mb rise. In (3.5) the factor of two takes into account the diffractive peak for each of the two protons while we only integrate over the region [$x \geq 0.8$, $M^2 \geq 2$ (GeV 2)] of the validity of Regge expansion. A rise of the small double-diffractive cross section should also be included in Fig. 11.¹⁰ As expected, the model with $\alpha_P(0) > 1$ produces a rising inelastic diffractive cross section as well as a rising total pp cross section.

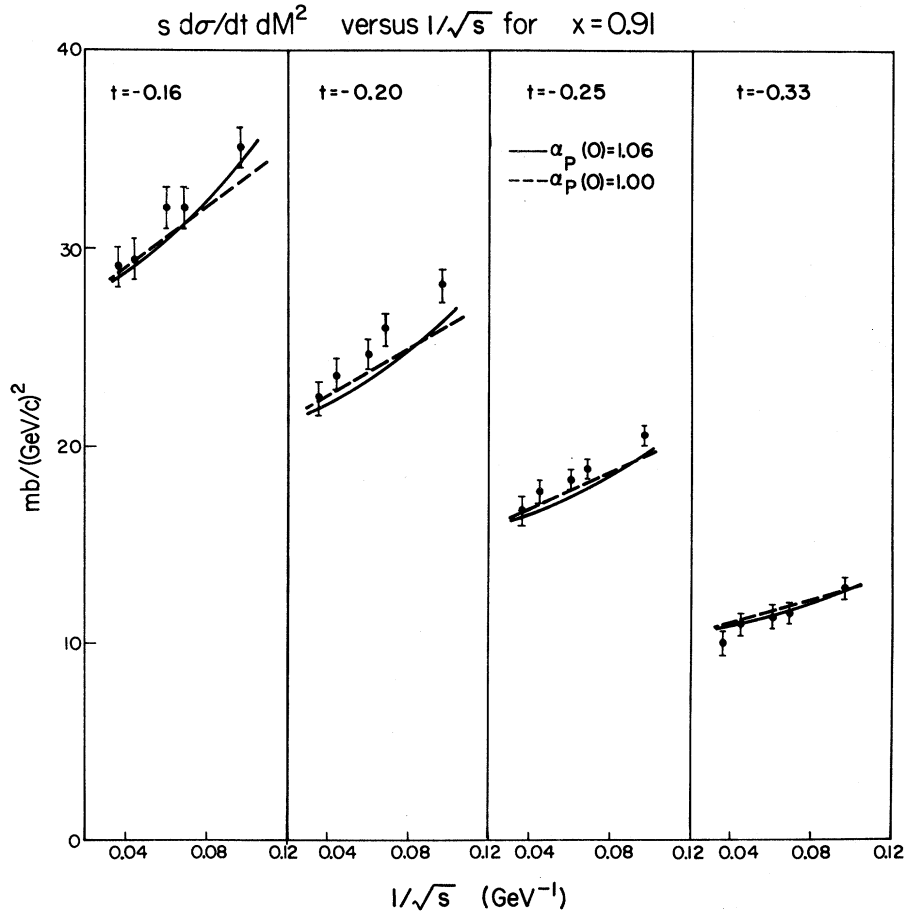


FIG. 8. Data on $s d\sigma/dt dM^2(pp \rightarrow p + X)$ versus $1/\sqrt{s}$ at fixed $x=0.91$ and $t=-0.16, -0.20, -0.25,$ and -0.33 (GeV/c)² from Ref. 36. The solid (dashed) curves are the result of Solution 2 with $\alpha_P(0)=1.06$ [Solution 1 with $\alpha_P(0)=1.0$].

where we have neglected the nondiffractive contributions from $G_{RRR}(t)$ and $G_{\pi\pi R}(t)$ and where $\nu_R = M_R^2 - t - m_p^2$, $M_R = \text{mass of } N^*$, $\nu_1 = \nu_R - 2M_R\Gamma$, $\nu_2 = \nu_R + 2M_R\Gamma$, $\Gamma = \text{width of } N^*$. The quantity d is a duality parameter which could in principle depend on t . If $d=1$ we have normal duality (i.e., resonances dual to Regge exchange), if $d=0$ we have extreme abnormal duality (i.e., resonances dual to Pomeron exchanges), and in between we have mixed duality. Given our present knowledge, the value of d is not known and in fact many authors argue over this point. Nevertheless, the energy dependence of $d\sigma/dt(pp \rightarrow pN^*)$ is not affected by the value of d and it is this energy dependence that is of great interest. Recent experimental data on $pp \rightarrow pN^*$ (1688) shows that the s dependence of the $N^*(1688)$ is remarkably similar to that of σ_{cl} , as explicitly demonstrated in Ref. 16. Thus to an excellent approximation σ_{cl} and σ_{N^*} are given by a single function of s which

can be reproduced by a bare Pomeron with $\alpha_P(0) > 1$.

It is amusing to note that the cross section for $N^*(1688)$ production is 0.56 ± 0.19 mb (Ref. 15) at $\sqrt{s} = 45$ GeV. Assuming $d=0$ in (3.6) and using our $G_{PPP}(t)$ from Solution 2 [$\alpha_P(0)=1.06$] yields a value of 0.48 mb, whereas Solution 1 with $\alpha_P(0)=1$ predicts 0.35 mb. This does not, of course, imply that $d=0$ but it does show that Eq. (3.6) together with a rising $pp \rightarrow pN^*$ cross section implies that $\alpha_P(0) > 1$. In a model with bare Pomeron intercept above unity both the elastic and diffractive cross sections are predicted to increase as s becomes large.

IV. ANALYSIS OF TOTAL-CROSS-SECTION AND ELASTIC-SCATTERING DATA

Having determined the triple-Regge couplings for a solution with $\alpha_P(0)=1.06$ we now attempt to fit the high-energy pp elastic³⁷ and total-cross-

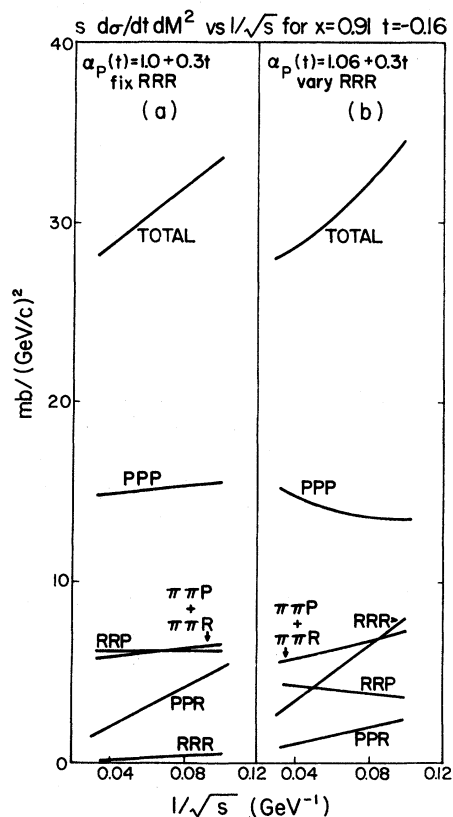


FIG. 9. Contributions to $s d\sigma/dt dM^2$ ($pp \rightarrow p + X$) versus $1/\sqrt{s}$ at $x=0.91$ and $t=-0.16$ (GeV/c)² from the various triple-Regge terms arising from Solution 1 with $\alpha_P(t)=1.0+0.3t$ [graph (a)] and Solution 2 with $\alpha_P(t)=1.06+0.3t$ [graph (b)].

section³⁸ data from ISR and Fermilab using the bare-Pomeron perturbation expansion (Fig. 1) and formulas (2.12), (2.13), and (2.14).

The bare Pomeron has trajectory $\alpha_P(t)=1.06+0.3t$. We take $r=0.1$ in (2.12) and fix $M_0^2=m_p^2$. The latter comes from our assumption that duality holds down to the elastic state. If we make the further assumption that $c_P=a_1$ in (2.12) (see Appendix C), we are left with the following five parameters: f_1, f_2, a_1, a_2 , and c_R . The values

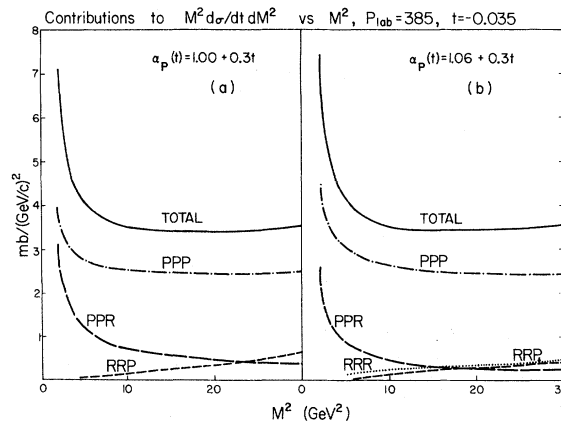


FIG. 10. Contributions to $M^2 d\sigma/dt dM^2$ ($p+p \rightarrow p+X$) versus M^2 at $t=-0.035$ (GeV/c)² and $p_{\text{lab}}=385$ GeV/c from the various triple-Regge terms arising from Solution 1 with $\alpha_P(t)=1.0+0.3t$ [graph (a)] and Solution 2 with $\alpha_P(t)=1.06+0.3t$ [graph (b)]. The RRR contribution to Solution 1 is small and not shown.

of these parameters resulting from a fit to the data are given in Table IV. Comparisons between the data and the resulting fit are shown in Figs. 12 and 13. The precise values chosen for r and M_0^2 are not crucial. The following comments are appropriate:

(a) The intercept of the Pomeron $\alpha_P(0)-1 \equiv \epsilon=0.06$ is mainly determined by the s dependence of the rising total cross section.

(b) The break at $t \approx -0.1$ (GeV/c)², as mentioned in Sec. II, is approximately determined by f_2 and a_2 , which supposedly parametrize the sum of the contributions of $(\pi\pi P)^2$ and $(RRP)^2$.

(c) The $(PPP)^2$ term is small and falls off as $|t|$ increases (owing to the assumption that $c_P \approx a_1$).

(d) The $(PPR)^2$ term rises as $|t|$ increases because of the factor $e^{2c_R t}$, $c_R > 0$. This is suggested by the large- $|t|$ behavior of the triple-Regge couplings $G_{PPR}(t)$ and $G_{RRP}(t)$ (see Table I and Appendix C).

(e) The dip at $t \approx -1.4$ (GeV/c)² comes from the destructive interference between the pole term

TABLE III. Values of the inelastic diffractive cross section $\sigma_D(s)$ (mb) [defined by (3.5)] arising from the PPP and PPR triple-Regge terms at $p_{\text{lab}}=300$ and 1500 GeV/c . Also shown is the difference $\Delta\sigma_D$ between these energies.

	$\sigma_D(300 \text{ GeV}/c)$		$\sigma_D(1500 \text{ GeV}/c)$		$\Delta\sigma_D$ PPP+PPR
	PPP	PPR	PPP	PPR	
FF Solution 1	3.90	2.42	4.81	1.94	0.44
$\alpha_P(0)=1.00$	4.68	1.49	5.81	1.22	0.87
$\alpha_P(0)=1.06$	4.86	0.94	6.87	0.87	1.93

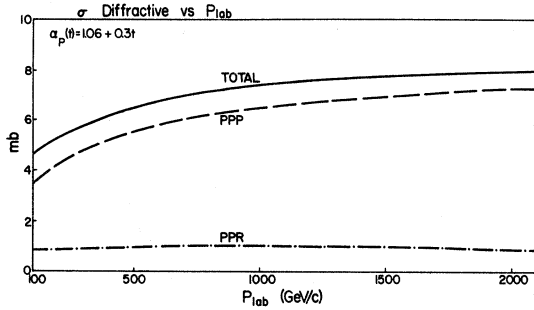


FIG. 11. Behavior of the inelastic diffractive cross section $\sigma_D(s)$ (mb) [defined by Eq. (3.5)] arising from the PPP and PPR and total=PPP+PPR triple-Regge terms of Solution 2 with $\alpha_P(t) = 1.06 + 0.3t$.

and the $(PPR)^2$ term. The position of the dip moves inward as s increases, because the ratio of the pole contribution to that of the $(PPR)^2$ term behaves like $s^{\alpha_P - \alpha_c} / \ln s = s^{-\epsilon + \alpha_P t / 2} / \ln s$, which decreases as s increases.

Our description of pp elastic scattering is similar in nature to the fits provided by Collins, Gault, and Martin,⁵ with the important exception that their work corresponds to the weak-coupling solution [$G_{PPP}(0) = 0$], whereas ours is a strong-coupling result [$G_{PPP}(0) \neq 0$]. They obtain a bare-Pomeron trajectory $\alpha_P(t) = 1.07 + 0.22t$ and reproduce the diffractive minimum as an interference between it and a "core" term. This "core" term is "explained" as a weak PP cut effect and is calculated by arbitrarily parameterizing the Gribov vertex (with increasing exponentials in $|t|$). $(PPR)^2$ bubble term is analogous to the "core" term of Collins, Gault, and Martin. We attempt to rationalize the needed t dependence of this term by observing the behavior of the triple-Regge couplings, however, both methods are equivalent since the Gribov vertex and the triple-Regge couplings can be related. In fact, in principle the fixed-pole residue at $t = 0$ (size of PP cut) can be obtained by taking the difference between even- and odd-moment FMSR from inclusive data.³⁹⁻⁴¹ As yet, the data do not seem to be sufficiently accurate to allow a reliable estimate though the authors of Ref. 36 do find the cuts to be smaller than would be obtained from a box diagram corresponding to the elastic pp intermediate state [Fig. 1(b)], which is what our results indicate.

The possibility of a bare-Pomeron intercept above unity has been examined in several recent works. Capella and Kaplan⁶ attempted an approximate summation of the bare perturbation expansion including higher-order terms and compared their results with the total-cross-section and pp

TABLE IV. Parameters determined by the total-cross-section and elastic-scattering data [$\epsilon = 0.1$, $M_0^2 = m_p^2$, $c_P = a_1$, $G_{PPP}(0) = 1.56$, $G_{PPR}(0) = 0.938$].

ϵ	0.06
f_1	19.0 mb GeV ²
$2a_1$	2.41 (GeV) ⁻²
f_2	8.21 mb GeV ²
$2a_2$	9.57 (GeV) ⁻²
$2c_R$	-1.99 (GeV) ⁻²

elastic-scattering data at $t = 0$ and obtained $\epsilon \approx 0.1$. Capella, Tran Thanh Van, and Kaplan⁶ further applied the bare perturbation expansion to πN , KN , and NN total cross sections and elastic-scattering data at $t = 0$, obtaining $\epsilon \approx 0.13$. In their calculation of the cut terms they have y diagrams whose t dependence at larger t needs to be investigated (we only have the bubble terms). Obviously more theoretical work is needed to understand the unknown t' dependence of the triple-Regge vertex [i.e., the b' parameter in (A1)].

V. SUMMARY AND CONCLUSIONS

We have performed a triple-Regge analysis of $pp \rightarrow pX$ with bare-Pomeron intercept above 1 and compared the results with fits using the more conventional $\alpha_P(0) = 1$. The triple-Regge couplings thus obtained are then used in the calculation of the elastic amplitude in the bare perturbation ex-

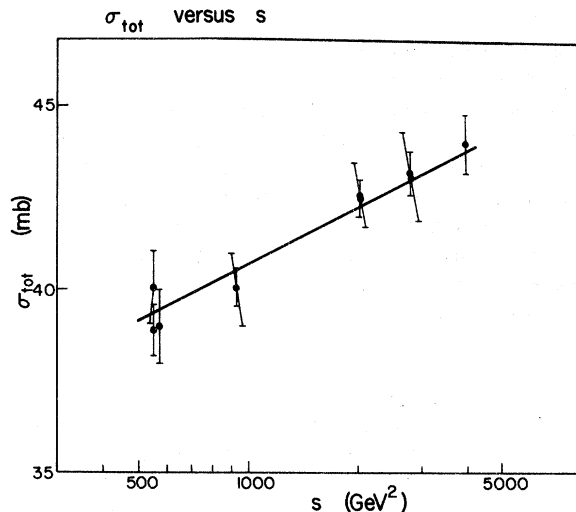


FIG. 12. Fit to the pp total cross section in the range $500 \leq s \leq 3000$ GeV² with a model that consists of a bare Pomeron with $\alpha_P(0) = 1.06$ and bubble-term corrections [Fig. 1(b)] calculated from the triple-Regge couplings of Solution 2. The data are from Ref. 38.

the case of the N^* (1688).

(g) Triple-Regge solutions with $\alpha_P(0) > 1$ produce a much greater rise in the total inelastic diffractive cross section over the ISR energy range (see Table III and Fig. 11).

(h) The triple-Regge couplings $G_{PPR}(t)$ and $G_{RRP}(t)$ do not behave like a single falling exponential (e^{bt}). In fact, both these couplings like to increase as $|t|$ increases for $|t| \geq 0.5$ (GeV/c)². This perhaps indicates the presence of helicity-flip couplings.

(i) One can get an adequate fit to the existing total pp cross-section and elastic data using this formalism.

(j) The s -channel approach has a simple interpretation in terms of a bare Pomeron and an absorptive correction generated by the contributions of various intermediate states $p + p \rightarrow X_1 + X_2$ including the elastic intermediate state.

(k) The break in $d\sigma/dt(pp \rightarrow pp)$ at small $|t|$ [$|t| \approx 0.1$ (GeV/c)²] may be attributable to the $(\pi\pi P)^2$ and $(RRP)^2$ bubble term contributions.

(l) The dip in $d\sigma/dt(pp \rightarrow pp)$ at large $|t|$ [$|t| \approx 1.4$ (GeV/c)²] may be attributable to the bare Pomeron interfering with the $(PPR)^2$ bubble term. However, it is necessary for the $(PPR)^2$ term to rise from its relatively small value at $t=0$ to a value large enough to produce this cancellation at $|t| \approx 1.4$ (GeV/c)². This interpretation does account for the slight movement of the dip inward as the energy increases.

From a theoretical viewpoint, our approach suffers from the following limitations:

(m) Once it is determined from the triple-Regge couplings that the bubble terms are small at $t=0$, then the precise values of these couplings do not play any role in determining the total pp cross-section behavior. The $\sigma_{\text{tot}}(pp)$ behavior is given primarily by the bare-Pomeron pole [with $\alpha_P(0) = 1.06$] and lower-lying Regge trajectory corrections.

(n) In general a triple-Regge vertex $g_{ijk}(t_1, t_2, t')$ depends on three variables. Our triple-Regge analysis determines this coupling when $t_1 = t_2 = t$ and $t' = 0$, whereas calculation of the bubble terms requires knowledge of g_{ijk} at $t_1 = t_2 = \frac{1}{2}t'$ with t' not necessarily vanishing. The triple-Regge analysis determines the bubble terms at $t=0$ only and there are unknown extrapolation factors (parameterized as e^{ct}) away from $t=0$. The cancellation between the $(PPR)^2$ bubble term and the bare Pomeron at $t = -1.4$ (GeV/c)² mentioned in (k) thus depends solely on this unknown extrapolation which must increase with $|t|$. It is suggestive, however, that since $G_{PPR}(t)$ increases as $|t|$ increases that this behavior might remain even when the presently unknown t dependences are included.

In view of the foregoing points we emphasize that in order to achieve further understanding of pp elastic scattering with our approach it is important to consider the following:

(o) The contributions of the bubble terms at $t=0$ are much smaller than what one would obtain from a box diagram corresponding to the elastic pp intermediate state by itself. To understand the difference one must consider in detail the inclusive sum rules which involve the fixed-pole residue in Reggeon-particle scattering. These residues, as is well known, are related to the Regge cuts.³⁹⁻⁴¹ Using existing data, however, little can be said at present concerning the size of the fixed-pole residues.

(p) In view of the necessity of having an increasing t behavior for the $(PPR)^2$ term, an understanding of the b' term in the exponent of the triple-Regge coupling is needed.⁴²

We note that the same formalism can be applied to other scattering processes to ascertain if any new and useful features emerge. Chu, Desai, and Stevens⁴³ have applied this approach to π^+p charge-exchange scattering with some success. Also one may need to introduce absorptive corrections for the inclusive scattering as in the present treatment of elastic scattering. This should be particularly important in the diffractive production of resonances where there is some evidence of a structure in t .⁴⁴

ACKNOWLEDGMENTS

It is a great pleasure to thank G. Van Dalen and Y. T. Oh for their help with the elastic data analysis. Two of us (S. -Y. C. and B. R. D.) would like to thank F. Hayot for collaboration in the initial stages of this work. In addition, R. D. F. would like to acknowledge useful discussions with P. Stevens and J. Kasman.

APPENDIX A: TRIPLE-REGGE VERTEX

Here we consider the t dependence of the triple-Regge vertex. In Fig. 3(a) we have described the triple-Regge vertex $g_{ijk}(t_1, t_2, t')$ defined in an exponential form as

$$g_{ijk}(t_1, t_2, t') = g_{ijk}(0) e^{b_i t_1 + b_j t_2 + b'_k t'}, \quad (\text{A1})$$

where i, j, k denote different trajectories. The prime in b'_k is present to emphasize that g_{ijk} is *not* symmetric in interchanges involving the subscript k (i.e., $g_{ijk} \neq g_{ikj}$, for instance) even if all the three trajectories are the same. This is a well-known result arising from the fact that the k channel corresponds to maximal helicity flip.

We will reserve the symbol a for the coupling between a Reggeon and external particles [see

Fig. 3(b)]; thus the particle-particle-Reggeon coupling will be given by

$$F_i(t) = F_i e^{\alpha_i t}. \quad (A2)$$

The conventional triple-Regge coupling used in the triple-Regge analyses is given by [see Fig. 3(c)]

$$\begin{aligned} G_{ijk}(t) &= \frac{F_i e^{\alpha_i t} F_j e^{\alpha_j t} F_k}{16\pi} g_{ijk}(t_1=t, t_2=t, t'=0) \xi_i \xi_j^* \\ &= \frac{F_i F_j F_k}{16\pi} g_{ijk}(0) e^{(\alpha_i + \alpha_j + \alpha_k)t} \xi_i \xi_j^*. \end{aligned}$$

In particular, we have for the *PPP* coupling

$$g_{PPP}(t_1, t_2, t') = g_{PPP}(0) e^{b_P t_1 + \bar{b}_P t_2 + b_P' t'}, \quad (A3)$$

$$G_{PPP}(t) = \frac{F_P^3 g_{PPP}(0)}{16\pi} e^{2(\alpha_P + b_P)t} \xi_P \xi_P^*,$$

whereas for the *PPR* coupling

$$g_{PPR}(t_1, t_2, t') = g_{PPR}(0) e^{\bar{b}_P t_1 + \bar{b}_P t_2 + b_P' t'}$$

and

$$G_{PPR}(t) = \frac{F_P^2 F_R g_{PPR}(0)}{16\pi} e^{2(\alpha_P + \bar{b}_P)t} \xi_P \xi_P^*.$$

Note that \bar{b}_P is, in general, different from b_P .

APPENDIX B: BUBBLE-TERM CALCULATIONS

Here we calculate the contribution of the bubble term [i.e., the second diagram in Figs. 1(a) and 1(b)], which in an *s*-channel picture involves the processes $p+p \rightarrow X_1+X_2 \rightarrow p+p$. The total contribution to the elastic amplitude can be written as

$$\frac{1}{s} \int \frac{dt_1 dt_2}{\sqrt{-\lambda}} \int dM_1^2 (M_1^2)^{\alpha_1(t)} \int dM_2^2 (M_2^2)^{\alpha_2(t)} e^{A_1 t_1 + A_2 t_2 + A' t} \left(\frac{s}{M_1^2 M_2^2} \right)^{\alpha(t_1) + \bar{\alpha}(t_2)}, \quad (B1)$$

where M_1 and M_2 are the invariant masses of X_1 and X_2 and the momentum transfer variables t_1 and t_2 correspond to the processes $p+p \rightarrow X_1+X_2$ and $X_1+X_2 \rightarrow p+p$, respectively, and where A_1, A_2 , and A' include the t dependence of the triple vertices. As we stated in Sec. II we will ignore the possibility of interference terms and, therefore, take $\alpha = \bar{\alpha} = \alpha_0$. We shall also consider only the cases where the trajectories α_1 and α_2 are both Pomerons or both Reggeons, so we take $\alpha_1 = \alpha_2 = \alpha$. (B1) now becomes

$$\frac{e^{A't}}{s} \int \frac{dt_1 dt_2}{\sqrt{-\lambda}} \int dM_1^2 (M_1^2)^{\alpha(t)} \int dM_2^2 (M_2^2)^{\alpha(t)} e^{A t_1 + A t_2} \left(\frac{s}{M_1^2 M_2^2} \right)^{\alpha_0(t_1) + \alpha_0(t_2)}. \quad (B2)$$

We can integrate over t_1 and t_2 , using the following formula valid for large s :

$$\int \frac{dt_1 dt_2}{\sqrt{-\lambda}} e^{B_1 t_1 + B_2 t_2} \approx \pi q \frac{\exp \left[(B_1 + B_2) t_{\min} + \frac{p'}{q} \left(\frac{B_1 B_2}{B_1 + B_2} \right) t \right]}{p' (B_1 + B_2)}, \quad (B3)$$

where q and p' are the center-of-mass momenta of the initial pp and the intermediate $X_1 X_2$ systems, respectively, and where t_{\min} is the minimum value of t_1 and t_2 :

$$t_{\min} = - \frac{(M_1^2 - m_p^2)(M_2^2 - m_p^2)}{s}, \quad (B4)$$

where m_p is the proton mass. The result is

$$\frac{\pi e^{A't}}{s} \left(\frac{q}{p'} \right) \int dM_1^2 (M_1^2)^{\alpha(t)} \int dM_2^2 (M_2^2)^{\alpha(t)} \left(\frac{s}{M_1^2 M_2^2} \right)^{2\alpha_0(0)} \frac{\exp[(p'/q)Bt/2 + 2Bt_{\min}]}{2B}, \quad (B5)$$

where

$$B = A + \alpha_0' \ln \left(\frac{s}{M_1^2 M_2^2} \right).$$

From (B4) and (B5) we notice that the exponential factor $e^{2Bt_{\min}}$ sharply reduces the contribution coming from the upper limit of M_1^2 and M_2^2 . This is the so-called " t_{\min} effect." One can, therefore, to a very good approximation, replace the upper limits of M_1^2 and M_2^2 by simply $(rs)^{1/2}$, where, with some average B ,

$$r \approx \frac{1}{2B} \ll 1, \quad (B6)$$

and we can safely assume

$$p' \approx q.$$

The contribution (B5) now reads

$$\frac{\pi e^{A't}}{s} \int_{M_0^2}^{(rs)^{1/2}} \frac{dM_1^2}{M_1^2} (M_1^2)^{\alpha(t)} \int_{M_0^2}^{(rs)^{1/2}} \frac{dM_2^2}{M_2^2} (M_2^2)^{\alpha(t)} \frac{e^{A't/2} (s/M_1^2 M_2^2)^{\alpha_{0c}(t)}}{2A + 2\alpha'_0 \ln(s/M_1^2 M_2^2)}, \quad (\text{B7})$$

where $\alpha_{0c}(t) = 2\alpha_0(0) - 1 + \frac{1}{2}\alpha'_0 t$ is the cut trajectory due to two α_0 trajectories.

(i) We first consider the bubble terms $(PPP)^2$ and $(PPR)^2$ where $\alpha_{0c} > \alpha$: We can make a further approximation, which reduces the integral in (B7) to an extremely simple form, by noticing that since M_1^2 and M_2^2 are much smaller than s throughout the integral, we can neglect $\ln(M_1^2 M_2^2)$ compared to $\ln s$ and take the denominator in (B7) out of the integral to obtain

$$\frac{\pi e^{A't} s^{\alpha_{0c}(t)}}{2A + 2\alpha'_0 \ln s} \int_{M_0^2}^{(rs)^{1/2}} \frac{dM_1^2}{M_1^2} (M_1^2)^{\alpha - \alpha_{0c}} \int_{M_0^2}^{(rs)^{1/2}} \frac{dM_2^2}{M_2^2} (M_2^2)^{\alpha - \alpha_{0c}} \quad (\text{B8})$$

$$= \frac{\pi e^{A't} s^{\alpha_{0c}(t)}}{2A + 2\alpha'_0 \ln s} \left[\frac{(rs)^{(\alpha - \alpha_{0c})/2} - (M_0^2)^{\alpha - \alpha_{0c}}}{\alpha - \alpha_{0c}} \right]^2. \quad (\text{B9})$$

The accuracy of the approximation made above in going from (B7) to (B8) depends on how fast the integrand falls off in M_1^2 and M_2^2 , which in turn depends on the value of $\alpha - \alpha_{0c}$:

$$\alpha - \alpha_{0c} = -\epsilon + \frac{1}{2}\alpha'_p t \quad \text{for } \alpha_0 = \alpha_p, \quad \alpha = \alpha_p, \quad (\text{B10})$$

$$\alpha - \alpha_{0c} = -\frac{1}{2} - 2\epsilon + (\alpha'_R - \frac{1}{2}\alpha'_p)t \quad \text{for } \alpha_0 = \alpha_p, \quad \alpha = \alpha_R. \quad (\text{B11})$$

Thus in general our approximation (B8) should be satisfactory. A possible exception to this could be the case (B10) at small t corresponding to the PPP term where because ϵ is very small the falloff in M_i^2 in (B8) given by $(M_i^2)^{-1-\epsilon}$ is not very sharp. However, the end product (B9) is algebraically so simple and its consequences to the amplitude so transparent that we shall continue to use our approximation also for the PPP term.

With the above approximation the contribution of the bubble diagrams are given by (apart from the normalization and signature factors)

$$e^{(2a_p + 2b_p' + b_p)t} \frac{s^{\alpha_c}}{4b_p + 2\alpha'_p \ln s} \left[\frac{(rs)^{(\alpha_p - \alpha_c)/2} - (M_0^2)^{\alpha_p - \alpha_c}}{\alpha_p - \alpha_c} \right]^2 \quad \text{for } \alpha_0 = \alpha_p, \quad \alpha = \alpha_p \quad (PPP), \quad (\text{B12})$$

$$e^{(2a_R + 2b_R' + b_P)t} \frac{s^{\alpha_c}}{4b_P + 2\alpha'_P \ln s} \left[\frac{(rs)^{(\alpha_R - \alpha_c)/2} - (M_0^2)^{\alpha_R - \alpha_c}}{\alpha_R - \alpha_c} \right]^2 \quad \text{for } \alpha_0 = \alpha_p, \quad \alpha = \alpha_R \quad (PPR),$$

where $\alpha_c = 1 + 2\epsilon + \frac{1}{2}\alpha'_p t$.

(ii) We now consider the bubble terms $(RRP)^2$ and $(\pi\pi P)^2$ where $\alpha_{0c} < \alpha$: In the integral (B7) we notice that if $\alpha_{0c} < \alpha$ then in contrast to the case (i) discussed earlier it is the upper limit $M_1^2 = (rs)^{1/2} = M_2^2$ which will dominate and hence one can replace $\ln(M_1^2 M_2^2)$ by $\ln(rs)$ in the denominator to obtain, instead of (B8) and (B9) the following:

$$\frac{\pi e^{A't} s^{\alpha_{0c}(t)}}{2A - 2\alpha'_0 \ln r} \int_{M_0^2}^{(rs)^{1/2}} \frac{dM_1^2}{M_1^2} (M_1^2)^{\alpha - \alpha_{0c}} \int_{M_0^2}^{(rs)^{1/2}} \frac{dM_2^2}{M_2^2} (M_2^2)^{\alpha - \alpha_{0c}} \quad (\text{B8}')$$

$$= \frac{\pi e^{A't} s^{\alpha_{0c}(t)}}{2A - 2\alpha'_0 \ln r} \left[\frac{(rs)^{(\alpha - \alpha_{0c})/2} - (M_0^2)^{\alpha - \alpha_{0c}}}{\alpha - \alpha_{0c}} \right]^2. \quad (\text{B9}')$$

We notice immediately that since $\alpha_{0c} = 2\alpha_0 - 1 + \frac{1}{2}\alpha'_0 t$ and $\alpha = 1 + \epsilon + \alpha'_p t$, for both the Reggeon ($\alpha_0 = \alpha_R$) and the pion ($\alpha_0 = \alpha_\pi$) one has $\alpha - \alpha_{0c} > 1$ for all values of t . Therefore, with negligible error, one can ignore the M_0^2 term to reduce (B9') to

$$C(t) s^{\alpha_p(t)}. \quad (\text{B9}'')$$

Therefore, the Reggeon and the pion bubble term simply "renormalize" the Pomeron residue function. We note that it is possible to have a very sharply falling $C(t)$ at $t=0$ because of the presence of the pion propagator term in $g_{\pi\pi P}$.

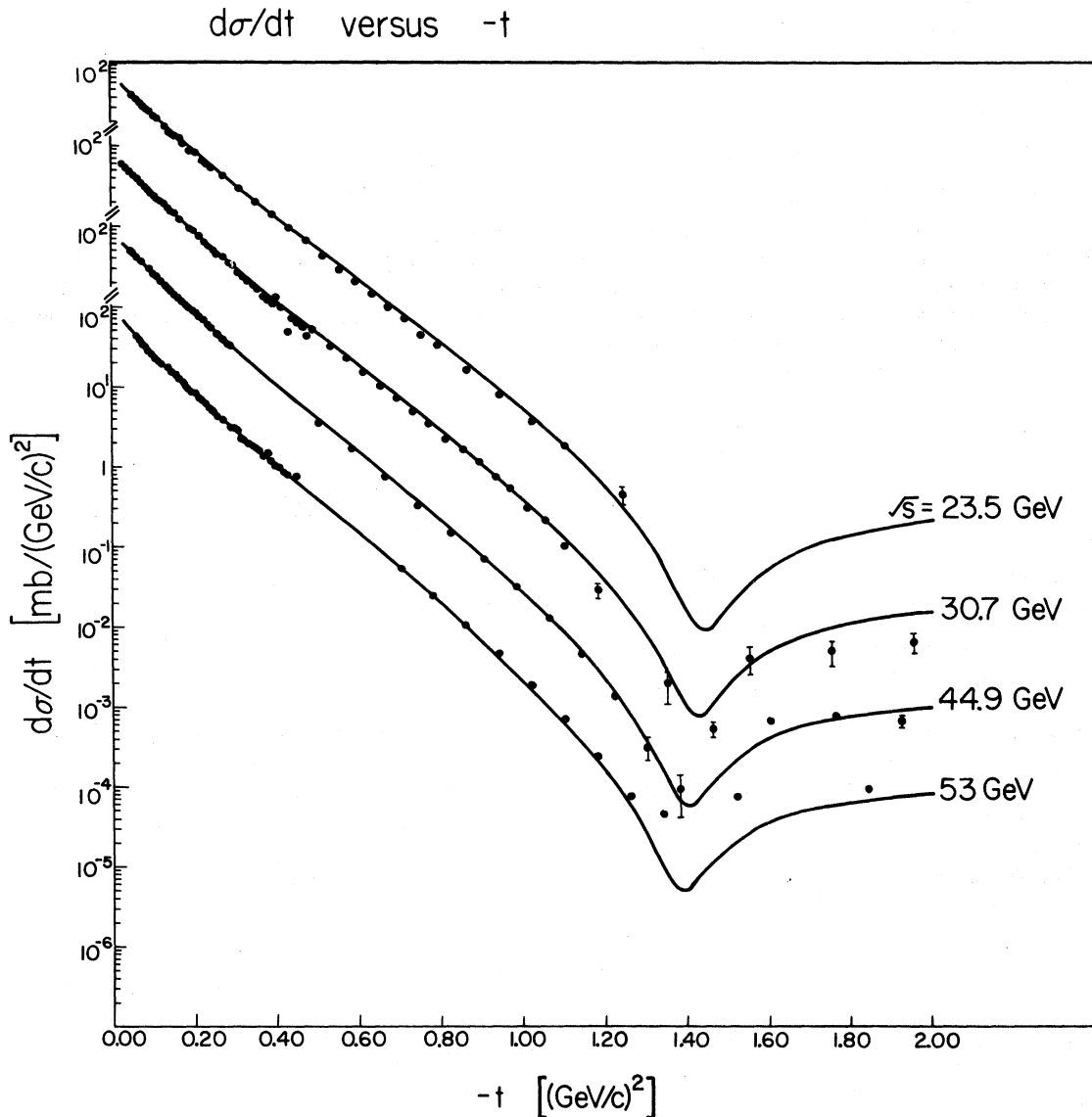


FIG. 13. Fit to the pp elastic differential cross section with a model that consists of a bare Pomeron with $\alpha_P(0) = 1.06$ and bubble-term corrections [Fig. 1(b)] calculated from the triple-Regge couplings of Solution 2. The data are from Ref. 37.

pansion shown in Fig. 1. We find the following:

- (a) The s dependence of σ_{tot} in the ISR range is consistent with $\alpha_P(0) = 1.06$.
- (b) Triple-Regge solutions with $\alpha_P(0) = 1.06$ are equally capable of fitting the existing $pp \rightarrow p + X$ high-energy inclusive data.
- (c) There is no indication of a vanishing of the triple-Pomeron coupling $G_{PPP}(t)$ down to $|t| \approx 0.035 \text{ (GeV/c)}^2$ (see Fig. 4).
- (d) There is evidence of some slight Pomeron shrinkage in inclusive $pp \rightarrow p + X$ scattering [$\alpha'_P \approx 0.3 \text{ (GeV/c)}^2$; see Fig. 5].

- (e) Triple-Regge solutions with $\alpha_P(0) > 1$ do not exhibit Feynmann scaling. They have the property that $sd\sigma/dt dM^2(pp \rightarrow p + X)$ at fixed x will decrease over the Fermilab energy range but instead of approaching a scaling limit (i.e., becoming independent of s) will start to increase in the ISR energy range as does $\sigma_{\text{tot}}(pp)$.

- (f) Triple-Regge solutions with $\alpha_P(0) > 1$ predict via FMSR and duality that diffractive resonance production, $pp \rightarrow p + N^*$, cross sections will mimic the $\sigma_{\text{el}}(pp)$ energy dependence (i.e., both will rise in the ISR range). This has in fact been seen for

APPENDIX C: $G_{ijk}(t) = \lambda_1 e^{b_1 t} + \lambda_2 e^{b_2 t}$

In Appendixes A and B the triple couplings were assumed to be single exponentials. However, in fitting $pp \rightarrow p + X$ inclusive data we find it necessary to parameterize the triple-Regge couplings as the sum of two exponentials [see (2.7) and Table I], the large- $|t|$ inclusive data requiring a flatter or even an increasing t dependence for some of the triple-Regge couplings. In this section we consider the consequences of such triple couplings to the elastic cross section. We will consider specifically, the $(PPP)^2$ and $(PPR)^2$ contributions.

If, instead of (A3), we write for the PPP coupling

$$g_{PPP}(t_1, t_2, t') = g_{PPP}^{(1)}(0) e^{b_P t_1 + b_P t_2 + b_P t'} + g_{PPP}^{(2)}(0) e^{d_P t_1 + d_P t_2 + b_P t'} \quad (C1)$$

and

$$G_{PPP}(t) = G_{PPP}^{(1)}(0) e^{2(a_P + b_P)t} + G_{PPP}^{(2)}(0) e^{2(a_P + d_P)t} \quad (C2)$$

then the triple-coupling contribution to the bubble term $(PPP)^2$ given by (B9) will instead be

$$e^{2(a_P + b_P)t} \left[\frac{g_{PPP}^{(1)2} e^{b_P t}}{4b_P + 2\alpha' \ln s} + \frac{2g_{PPP}^{(1)} g_{PPP}^{(2)} e^{(b_P + d_P)t/2}}{2(b_P + d_P) + 2\alpha' \ln s} + \frac{g_{PPP}^{(2)2} e^{d_P t}}{4d_P + 2\alpha' \ln s} \right] \quad (C3)$$

From the knowledge of G_{PPP} given in Table I and of $a_P (= a_1)$ in Table IV we obtain (in GeV^{-2})

$$a_P = 2.4, \quad b_P = 0.54, \quad d_P = -0.43.$$

Thus in view of the smallness of b_P and d_P the sum inside the square brackets in (C3) will be essentially a constant in t . The value of b_P cannot be determined from inclusive analysis since the G 's correspond to $t' = 0$. However, the factor $e^{(a_P + b_P)t}$ is, for fixed t_1 and t_2 , the residue function for the maximal helicity-flip amplitude for Pomeron-proton scattering, which will most likely be a decreasing function of $|t|$. Therefore, it is reasonable to expect (C3) to be an exponentially decreasing function in t . In order to have as few parameters as possible we will assume the square-bracketed terms in (C.3) to be simply $1/2\alpha' \ln s$. It is under these assumptions that we have written the expression for the $(PPP)^2$ contribution to the elastic amplitude in (2.12). We have further as-

sumed $b'_P = 0$ to minimize the number of parameters (see Table IV).

For the PPR coupling, if instead of (A4) we write

$$g_{PPR}(t_1, t_2, t') = g_{PPR}^{(1)}(0) e^{\bar{b}_P t_1 + \bar{b}_P t_2 + b'_R t'} + g_{PPR}^{(2)}(0) e^{\bar{d}_P t_1 + \bar{d}_P t_2 + b'_R t'} \quad (C4)$$

and

$$G_{PPR}(t) = G_{PPR}^{(1)}(0) e^{2(a_P + \bar{b}_P)t} + G_{PPR}^{(2)}(0) e^{2(a_P + \bar{d}_P)t},$$

then the triple-coupling contribution to the bubble term $(PPR)^2$ will be, instead of (B9),

$$e^{2(a_R + b'_R)t} \left[\frac{g_{PPR}^{(1)2} e^{\bar{b}_P t}}{4\bar{b}_P + 2\alpha' \ln s} + \frac{2g_{PPR}^{(1)} g_{PPR}^{(2)} e^{(\bar{b}_P + \bar{d}_P)t/2}}{2(\bar{b}_P + \bar{d}_P) + 2\alpha' \ln s} + \frac{g_{PPR}^{(2)2} e^{\bar{d}_P t}}{4\bar{d}_P + 2\alpha' \ln s} \right] \quad (C5)$$

From G_{PPR} given in Table I we obtain (in GeV^{-2})

$$\bar{b}_P = 0.33, \quad \bar{d}_P = -2.0.$$

We note that in contrast to PPP we have a very large rising exponential term in the square brackets in (C5). The denominator of the third term is negative for the s values of interest. This is so because we have incorrectly integrated up to $t = -\infty$. When the correct finite upper limit is chosen, appropriate to the range in t of our analysis, one finds the denominator to be positive but very small. Thus the third term is, indeed, quite large and rising.

In addition, we note that for fixed masses t_1 and t_2 , $e^{(a_R + b'_R)t}$ is the residue function for the maximal helicity-flip amplitude for elastic Pomeron-proton scattering with Reggeon exchange. Generally, the helicity-flip amplitudes have slower decrease in $|t|$ compared to the non-helicity-flip amplitudes. Furthermore, residues for Reggeon exchange fall more slowly in $|t|$ than those for the Pomeron exchange. We anticipate, therefore, that $(a_R + b'_R)$ is quite small. It is then plausible that the *entire* expression in (C5) can be given by a *rising* exponential. In our phenomenological expression (2.12) we have approximated (C5) by a single term

$$\frac{e^{2c_R t}}{2\alpha' \ln s}$$

and the fact that c_R is found to be negative from the elastic data is perhaps not too surprising.

*Work supported in part by the United States Energy Research and Development Administration and the National Science Foundation.

†On leave from Indiana University, Bloomington,

Indiana 47401.

‡On sabbatical leave during academic year 1975-1976 at CERN, Geneva, Switzerland.

§H. Cheng and T. T. Wu, Phys. Rev. Lett. 24, 1456

- (1970); J. L. Cardy, Nucl. Phys. **B28**, 455 (1971); **B28**, 477 (1971); H. Cheng, J. K. Walker, and T. T. Wu, Phys. Lett. **44B**, 97 (1973); **44B**, 283 (1973).
- ²T. T. Chou and C. N. Yang, Phys. Rev. **170**, 1591 (1968).
- ³T.-Y. Cheng, S.-Y. Chu, and A. W. Hendry, Phys. Rev. **D 6**, 190 (1972).
- ⁴M. Kal, Nucl. Phys. **B62**, 402 (1973).
- ⁵P. D. B. Collins, F. D. Gault, and A. Martin, Nucl. Phys. **B80**, 135 (1974); A. Martin, Nucl. Phys. **B77**, 226 (1974); P. D. B. Collins, F. D. Gault, and A. Martin, Nucl. Phys. **B83**, 241 (1974).
- ⁶A. Capella and J. Kaplan, Phys. Lett. **52B**, 448 (1974); A. Capella, J. Tran Thanh Van, and J. Kaplan, Nucl. Phys. **B97**, 493 (1975).
- ⁷J. S. Ball and F. Zachariassen, Nucl. Phys. **B85**, 317 (1975).
- ⁸J. Dias de Deus, Nucl. Phys. **B59**, 231 (1973); V. Barger, V. Barger, J. Luthe, and R. J. N. Phillips, *ibid.* **B88**, 237 (1975).
- ⁹For a review see V. Barger, in *Proceedings of the XVII International Conference on High Energy Physics, London, 1974*, edited by J. R. Smith (Rutherford Laboratory, Chilton, Didcot, Berkshire, England, 1974), p. I-193.
- ¹⁰D. P. Roy and R. G. Roberts, Nucl. Phys. **B77**, 240 (1974).
- ¹¹R. D. Field and G. C. Fox, Nucl. Phys. **B80**, 367 (1974).
- ¹²G. C. Fox, in *High Energy Collisions—1973*, proceedings of the Fifth International Conference, Stony Brook, edited by C. Quigg (A.I.P., New York, 1973), p. 180.
- ¹³For a discussion as to the status of duality in Reggeon-particle scattering see P. Hoyer, in *Proceedings of the XVII International Conference on High Energy Physics, London, 1974*, edited by J. R. Smith (Ref. 9), p. I-158.
- ¹⁴E. Nagy, M. Regler, W. Schmidt-Parzefall, K. Winter, A. Brandt, G. Flüge, F. Niebergall, K. R. Schubert, P. E. Schumacher, C. Broll, G. Coignet, J. Favier, L. Bassonet, M. Vivargrat, W. Bartl, H. Dibon, Ch. Gottfried, and G. Neuhofer, paper submitted to the XVII International Conference on High Energy Physics, London, 1974 (unpublished).
- ¹⁵R. Webb, G. Trilling, V. Telegdi, P. Strolin, B. Shen, P. Schlein, J. Rander, B. Naroska, T. Meyer, W. Marsh, W. Lockman, J. Layter, A. Kernan, M. Hansroul, S.-Y. Fung, H. Foeth, R. Ellis, A. Der-evshikov, M. Bozzo, A. Böhm, and L. Baksay, Phys. Lett. **55B**, 331 (1975).
- ¹⁶B. R. Desai and B. C. Shen, Univ. of California, Riverside, Report No. UCR-75-01 (unpublished).
- ¹⁷V. N. Gribov, Zh. Eksp. Teor. Fiz. **53**, 654 (1967); [Sov. Phys.—JETP **26**, 414 (1968)].
- ¹⁸V. N. Gribov and A. A. Migdal, Yad. Fiz. **8**, 1002 (1968) [Sov. J. Nucl. Phys. **8**, 583 (1969)].
- ¹⁹A. A. Migdal, A. M. Polyakov, and K. A. Ter-Martirosyan, Phys. Lett. **48B**, 239 (1974); Report No. ITEP-102, 1973 (unpublished); H. D. I. Abarbanel and A. B. Bronzan, Phys. Lett. **48B**, 345 (1974); Phys. Rev. **D 9**, 2397 (1974).
- ²⁰J. B. Bronzan, Phys. Rev. **D 4**, 1097 (1971).
- ²¹R. L. Sugar and A. R. White, Fermilab Report No. 74/75 THY, 1974 (unpublished); A. R. White, Fermilab Report No. Conf-74/77-THY, 1974 (unpublished).
- ²²H. D. I. Abarbanel, J. B. Bronzan, R. L. Sugar, and A. R. White, Phys. Rep. **216**, 119 (1975).
- ²³Y. Akimov, L. Golovanov, S. Mukhin, G. Takhtamyshev, V. Tsarev, E. Malamud, R. Yamada, P. Zimmerman, R. Cool, K. Goulianos, H. Sticker, D. Gross, A. Melissinos, D. Nitz, and S. Olsen, Phys. Rev. Lett. **35**, 766 (1975).
- ²⁴B. R. Desai, Phys. Lett. **50B**, 494 (1974).
- ²⁵M. Bishari and J. Koplik, Phys. Lett. **44B**, 175 (1973); W. R. Frazer, D. R. Snider, and C.-I. Tan, Phys. Rev. **D 8**, 3180 (1973). In contrast to the Reggeon field theory, these authors use the positive sign for the Pomeron-Pomeron cut.
- ²⁶One can accomplish this in the standard manner (see Ref. 25) by using the j -plane language and the factor $e^{-(j-\alpha_0)n\Delta}$ for the production of $n+1$ fireballs, where $\Delta = \ln \bar{s}$.
- ²⁷The proper signature is inserted by the replacement $s \rightarrow se^{-i\pi/2}$ [see Appendixes A, B and (2.12)].
- ²⁸The bubble terms $(\pi\pi P)^2$ and $(RRP)^2$ are, in fact, double poles which have the form $(a+b \ln s)$. For our purposes we have suppressed the $\ln s$ dependence by approximating it by a constant (see also Appendix B). Furthermore, in Reggeon field theory the "bare" term presumably already contains the pion and Reggeon bubble contributions and consequently it will have a form more complicated than our (2.3) and (2.4). For phenomenological simplicity, however, we have chosen to parametrize the total contribution as the sum of (2.3) and (2.11) [see the first term in (2.12)].
- ²⁹R. Schanberger, J. Lee-Franzini, R. McCarthy, S. Childress, and P. Franzini, report, 1973 (unpublished).
- ³⁰This data was withdrawn by J. Lee-Franzini at the XVII International Conference on High Energy Physics, London, 1974.
- ³¹R. McCarthy (private communication).
- ³²F. K. Loebinger (private communication).
- ³³For further discussion of the new $pd \rightarrow d + X$ data and other attempts to fit the data using the triple-Regge formalism see Refs. 34 and 35.
- ³⁴S. V. Mukhin and V. A. Tsarev, in *Particles and Fields—1974*, proceedings of the 1974 Williamsburg meeting of the Division of Particles and Fields of the American Physical Society, edited by Carl E. Carlson (A.I.P., New York, 1975), p. 263.
- ³⁵V. A. Tsarev, Phys. Rev. **D 11**, 1875 (1975).
- ³⁶K. Abe, T. DeLillo, B. Robinson, F. Sannes, J. Carr, J. Keyne, and I. Siotis, paper submitted to the Berkeley Meeting of the Division of Particles and Fields of the A.P.S., 1973 (unpublished).
- ³⁷G. Barbiellini *et al.*, Phys. Lett. **39B**, 663 (1972); A. Bohm *et al.*, *ibid.* **49B**, 491 (1974).
- ³⁸U. Amaldi *et al.*, Phys. Lett. **44B**, 112 (1973); **43B**, 231 (1973); S. R. Amendolia *et al.*, *ibid.* **44B**, 119 (1973); G. Bellettini *et al.*, Nucl. Phys. **B69**, 336 (1974); H. R. Gustafson *et al.*, Phys. Rev. Lett. **32**, 441 (1974); C. Bromberg *et al.*, Phys. Rev. Lett. **31**, 1563 (1973); V. Bartenev *et al.*, *ibid.* **31**, 1088 (1973); **31**, 1367 (1973).
- ³⁹V. N. Gribov, Zh. Eksp. Teor. Fiz. **53**, 654 (1967) [Sov. Phys.—JETP **26**, 414 (1968)].
- ⁴⁰D. P. Roy and R. G. Roberts, Phys. Lett. **40B**, 555 (1972).
- ⁴¹I. J. Muzinich, F. E. Paige, T. L. Trueman, and L.-L.

Wang, Phys. Rev. 6, 1048 (1972).

⁴²C. Sorensen, Phys. Rev. D 6, 2554 (1972).

⁴³S. Y. Chu, B. R. Desai, and P. R. Stevens following paper, Phys. Rev. D 13, 2985 (1976).

⁴⁴G. L. Kane, Acta Phys. Polon. B3, 845 (1973); H. I. Miettinen, in *High Energy Hadronic Interactions*, pro-

ceedings of the first session of the IX Rencontre de Moriond, 1974, edited by J. Tran Thanh Van (Université de Paris-Sud, Orsay, 1974).

⁴⁵S. J. Barish, D. C. Colley, P. F. Schultz, and J. Whitmore, Phys. Rev. Lett. 31, 1080 (1973).